Optimized control and simulation of a grid-integrated photovoltaic and fuel cell hybrid power system

Amal Satif, Laamari Hlou, Rachid Elgouri

Laboratory of Advanced Systems Engineering, National School of Applied Sciences (ENSA), Kenitra, Morocco

Article Info	ABSTRACT

In this study, we propose an advanced power control strategy tailored for a grid-connected photovoltaic-hydrogen hybrid system aimed at ensuring reliable energy supply to consumers. This hybrid system integrates photovoltaic (PV) panels as the primary energy source supplemented by hydrogen fuel production through electrolysis of surplus PV-generated electricity. To optimize system flexibility and efficiency, we employ several advanced control techniques. A novel maximum power point tracking (MPPT) method, enhanced with a proportional-integral (PI) controller, surpasses conventional perturb and observe (P&O) techniques to maximize PV power output. For precise control of the three-phase photovoltaic inverter, we utilize a space vector pulse width modulation (SVPWM) algorithm. Synchronization with the utility grid is ensured by a phase-locked loop (PLL), maintaining phase coherence between the inverter output and grid supply. The primary goal is to develop a comprehensive and efficient control strategy for grid-connected hybrid systems, addressing both energy generation and storage challenges. MATLAB simulations validate the system's performance, demonstrating high energy conversion efficiency and robust control across varying conditions. This study underscores the potential of hybrid PV-hydrogen systems to provide sustainable and resilient energy solutions for future grid integration.

Corresponding Author:

Amal Satif
Laboratory of Advanced Systems Engineering, National School of Applied Sciences (ENSA)
Kenitra, Morocco
Email: amal.satif@uit.ac.ma

1. INTRODUCTION

The global energy supply is heavily dependent on fossil fuels and nuclear resources, which pose significant environmental threats, including atmospheric pollution, greenhouse gas emissions, and nuclear fallout. These challenges contribute to climate change, now recognized as a critical global issue impacting sustainability, human health, and economic stability [1]. Furthermore, the depletion of fossil fuel reserves, rising energy costs, and the uncertainty surrounding oil and natural gas supplies underscore the urgent need for alternative, sustainable energy sources [2].

To meet these challenges, renewable energy technologies are increasingly adopted to ensure long-term energy security. However, one of the major constraints for grid-connected systems relying on renewable sources is overcoming intermittency to ensure a continuous and reliable power supply [2]. Addressing this issue requires integrating advanced energy storage technologies into renewable energy systems [3].

Hybrid grid-connected systems present a promising solution by combining renewable energy generation with effective storage mechanisms to regulate and stabilize energy supply. This research focuses on the production of solar fuels, specifically solar hydrogen, which chemically stores solar energy. Hydrogen

is abundant, clean, and, when used in fuel cells (FCs), produces no pollutants, making it an ideal energy carrier for grid-connected systems [4]. Among various hydrogen production methods, proton exchange membrane (PEM) electrolyzers stand out due to their compact design, absence of harmful chemicals, and ability to generate high-purity hydrogen suitable for direct use in FCs [5].

While numerous studies have explored the performance of individual components, such as PEM electrolyzers, photovoltaic (PV) panels, and FCs, there is a significant gap in the literature when it comes to integrating these components into a unified grid-connected hybrid system. Research such as [6]–[10] has primarily focused on evaluating standalone elements, without addressing the complex challenges of control and integration within a grid-connected framework. Other works have concentrated on the physical behavior of cells or stacks [11], [12], yet do not fully consider the dynamic interactions between PV systems, electrolyzers, and FCs required for optimal performance in hybrid systems. Additionally, the role of power electronics—such as DC/DC converters, three-phase inverters, filters, and transformers—is crucial in enhancing system efficiency and deserves more attention [13], [14].

Our study bridges key gaps by presenting a comprehensive integration of PV and hydrogen FC systems in a grid-connected framework. We emphasize holistic design, incorporating advanced maximum power point tracking (MPPT) for PV optimization, effective PEM electrolyzer management, space vector pulse width modulation (SVPWM) for precise inverter control, and phase-locked loop (PLL) synchronization for seamless grid operation. This approach enhances system reliability, energy efficiency, and adaptability, offering a robust solution for sustainable hybrid energy systems in real-world applications [15].

The primary objectives of this study are as follows: i) Design and integration of a hybrid system develop a grid-connected hybrid power system that integrates PV panels and hydrogen FC generators; ii) Optimization of control strategies implement advanced control strategies to optimize the power output from both the PV panels and the FC generator, ensuring efficient grid synchronization; and iii) Simulation and validation conduct extensive simulations to evaluate the hybrid system's performance under various operating conditions and validate the effectiveness of the proposed control strategies. By addressing these objectives, this study aims to advance the state of knowledge in hybrid renewable energy systems and provide solutions for integrating clean energy technologies into grid-connected systems.

The structure of this work is as follows: section 2 presents an overview of the power system and its components. Section 3 focuses on the comprehensive implementation of the PV/FC hybrid grid-connected system, covering the control techniques and components utilized. Section 4 details the obtained results, while section 5 concludes the paper and explores potential avenues for future research.

2. POWER SYSTEM OVERVIEW AND COMPONENTS

This study evaluates the performance of a grid-connected hybrid PV and hydrogen FC system through simulations. The setup comprises a 5 kW PV array, a 1 kW PEM electrolyzer, and a 1 kW hydrogen FC, managed by an enhanced perturb and observe (P&O) MPPT control algorithm. MATLAB-Simulink models the components under varying irradiance and temperature, simulating real-world conditions. Experimental data, including voltage, current, and power output, are analyzed to assess energy efficiency, system stability, and load response. Figure 1 outlines the system's interconnected components, with subsequent subsections detailing their functionalities.
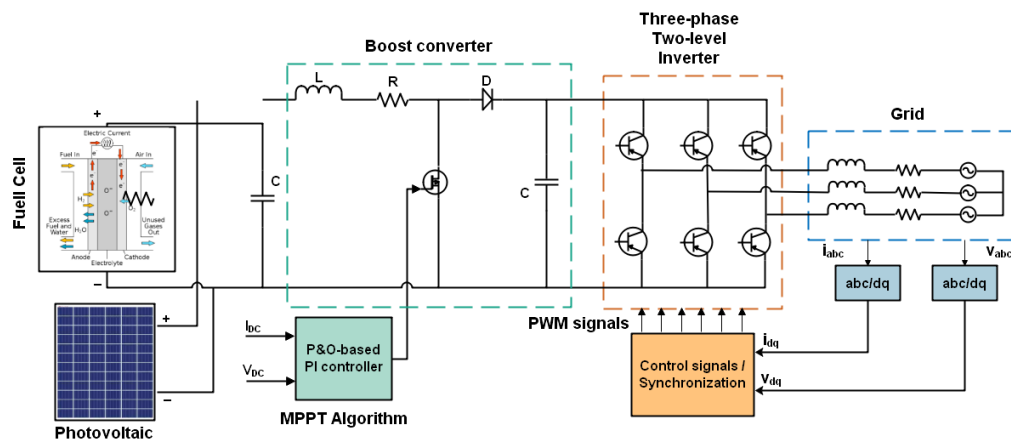
Figure 1. PV/FC proposed system connected to grid

2.1. Photovoltaic panel model

Figure 2 illustrates a solar cell model. The solar panel is configured with N_s cells in series to increase voltage and N_p cells in parallel to enhance current. The conversion of solar energy into electrical energy is described by the non-linear (1) [16].

$$I_{pv} = I_{ph} - I_o \left[exp \left(\frac{V_{pv}+R_S I_{pv}}{V_t a} \right) - 1 \right] - \frac{V_{pv}+R_S I_{pv}}{R_{sh}} \tag{1}$$

where I_{pv} is the PV generated current, V_{pv} is the PV generated voltage, I_{ph} is the photo-current, I_0 is the saturated diode current, q is the electron charge, k is Boltzmann's constant, a is an ideality factor (varies between 1.2 and 5), and T is the absolute cell temperature.
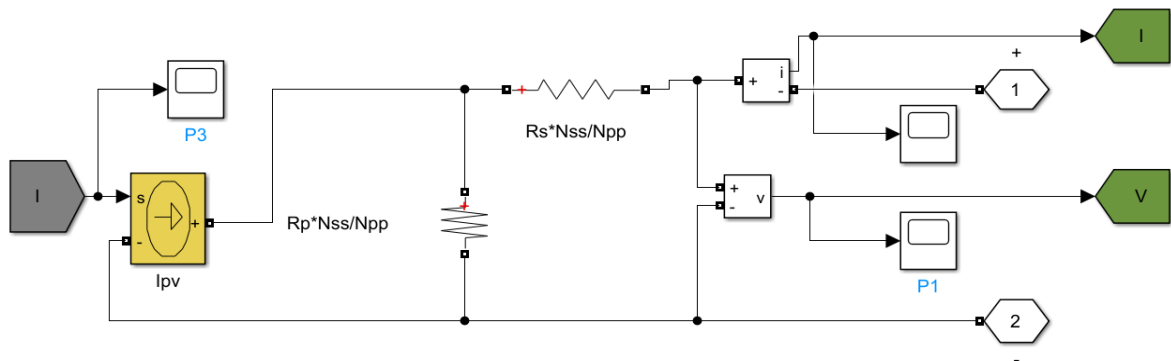
Figure 2. Solar cell modeling

The expressions for photo-current I_{ph} and saturation current I_0 are defined by (2) and (3) [17]:

$$I_{ph} = (I_{sc} + K_i dT) \frac{G}{G_n} \tag{2}$$

$$I_o = \frac{I_{sc} + K_i dT}{exp \left[\frac{V_{oc} + K_v dT}{V_t a} \right] - 1} \tag{3}$$

where $V_t = \frac{K^* T^* N_s}{q}$. The selected PV module is KC200GT. The characterizing parameters are taken from the system advisory model. It can be found in Table 1 [17].

Table 1. Electrical characteristic of KC200GT panel.

Parameter	Value
Short-circuit current I_{sc} (A)	8.2
Open circuit voltage V_{oc} (V)	32.9
Cells per module Ns	54
K_i (A/°C)	3e^{-3}
K_v (V/°C)	-120
Nominal temperature (°C)	25

2.2. Boost converter

The solar generator's output voltage is often insufficient for many applications, and maximizing energy conversion efficiency requires operating near the PV source's maximum power point. However, output power fluctuates due to variations in solar radiation, temperature, and load characteristics, resulting in inconsistent power delivery. To mitigate this, a DC/DC converter, regulated by an MPPT algorithm [18], is implemented between the renewable sources and the load. Figure 3 illustrates the proposed system, integrating a PV/FC generator with a DC-DC boost converter and MPPT algorithm to optimize power tracking.
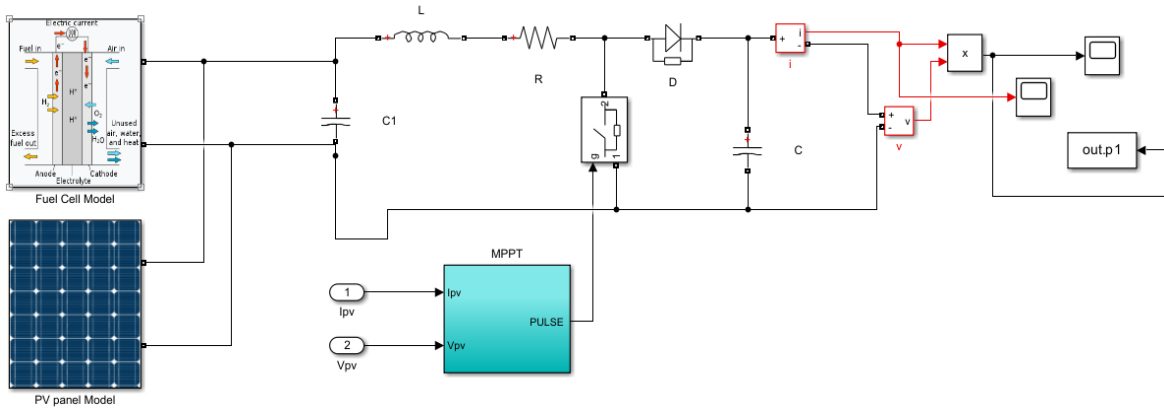
Figure 3. Block diagram of the Boost converter

2.3. PEM electrolyzer model

Water electrolysis decomposes the molecules of water into hydrogen and oxygen. The electrochemical reactions in the PEM electrolyzer, triggered by an applied potential, are shown in (4) and (5). Figure 4 illustrates the fundamental principle of a water electrolyzer [19].

$$\text{Anode: } H_2O \rightarrow 2H^+ + \frac{1}{2}O_2 + 2e^- \tag{4}$$

$$\text{Cathode: } 2H^+ + 2e^- \rightarrow H_2 \tag{5}$$

In the electrolyzer, water at the anode is split into oxygen gas, electrons, and protons. The protons move to the cathode through a PEM, while electrons travel via an external circuit, driving the reaction. At the cathode, electrons and protons recombine to form hydrogen gas. Continuous water supply to the membrane electrode is essential, as is the removal of hydrogen and oxygen. The reactions occur at the membrane-electrode interface, necessitating the porous electrode to facilitate water flow to the catalyst layer and gas removal from reaction sites. The PEM electrolyzer cell model comprises four principal components: anode, cathode, membrane, and voltage [20].
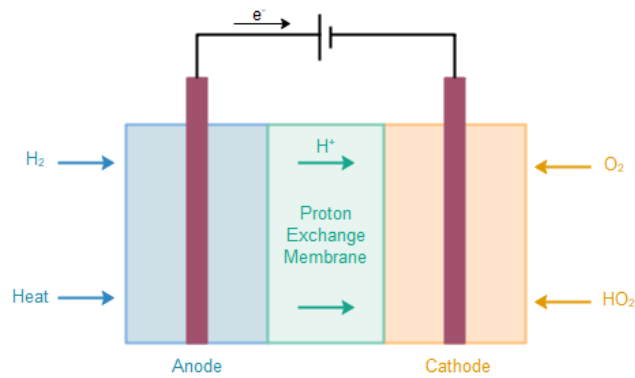
Figure 4. PEM fuel cell representation

2.3.1. Anode ancillary

The anode ancillary manages the calculation of oxygen and water flows and their partial pressures. At the anode, according to (4), water is oxidized to produce oxygen gas, protons, and electrons. The equations for these reactions are provided [21].

$$\frac{dN_{O_2}}{dt} = \dot{N}_{O_{2_{ai}}} - \dot{N}_{O_{2_{ao}}} + \dot{N}_{O_{2_{gn}}} \tag{6}$$

$$\frac{dN_{H_2O}}{dt} = \dot{N}_{H_2O_{ai}} - \dot{N}_{H_2O_{ao}} - \dot{N}_{H_2O_{eod}} + \dot{N}_{H_2O_{diff}} \tag{7}$$

where, $\dot{N}_{O_{2_{ai}}}$, $\dot{N}_{O_{2_{ao}}}$, $\dot{N}_{H_2O_{ai}}$, $\dot{N}_{H_2O_{ao}}$ (mol/s) are inlet and outlet molar flows of oxygen and water anode, respectively. $\dot{N}_{H_2O_{eod}}$ and $\dot{N}_{H_2O_{diff}}$ are electro-osmatic drag and diffusion flows. $\dot{N}_{O_{2_{gn}}}$ is the molar flow rate of oxygen generation at the anode. The oxygen molar flux through the anode, using Faraday's law, is given by (8) [21].

$$n_{O_2} = \frac{\dot{N}_{O_{2_{gn}}}}{A} = \frac{I}{4FA} \tag{8}$$

2.3.2. Cathode ancillary
The cathode ancillary determines the flow rates and partial pressures of hydrogen and water. Hydrogen ions interact with electrons supplied by the power source to produce hydrogen gas. The equations governing the cathode ancillary are (9) and (10) [20].

$$\frac{dN_{H_2}}{dt} = \dot{N}_{H_{2_{ci}}} - \dot{N}_{H_{2_{co}}} + \dot{N}_{H_{2_{gn}}} \tag{9}$$

$$\frac{dN_{H_2O}}{dt} = \dot{N}_{H_2O_{ci}} - \dot{N}_{H_2O_{co}} - \dot{N}_{H_2O_{eod}} + \dot{N}_{H_2O_{diff}} \tag{10}$$

The molar flux of hydrogen at the cathode can be expressed, using Faraday's law, as in (11).

$$n_{H_2} = \frac{\dot{N}_{H_{2_{gn}}}}{A} = \frac{I}{2FA} \tag{11}$$

2.3.3. Membrane ancillary
The membrane electrode assembly is the core of the PEM electrolyzer, involving diffusion, electro-osmotic drag, and hydraulic pressure effects [19].

$$\dot{N}_{H_2O_m} = \dot{N}_{H_2O_{diff}} - \dot{N}_{H_2O_{eod}} + \dot{N}_{H_2O_{hpe}} \tag{12}$$

The rate of water transport due to diffusion can be described by Fick's laws of diffusion [21].

$$\dot{N}_{H_2O_{diff}} = \frac{AD_{wm}}{a_m} \left(C_{H_2O,m,a} - C_{H_2O,m,c} \right) \tag{13}$$

where, D_{wm} is the membrane diffusion coefficient of water, a_m is the membrane thickness, $C_{H_2O,m,a}$, and $C_{H_2O,m,c}$ represent the concentrations of water at the membrane sides.
Electro-osmotic drag is dependent on the flow of hydrated protons:

$$\dot{N}_{H_2O_{eod}} = \frac{n_d\, i\, A}{F} \tag{14}$$

where n_d is the electro-osmotic drag coefficient. Experimentally, n_d varies with cathode pressure, current density, and temperature. Water transport from cathode to anode through the membrane is described by Darcy's law [21]:

$$\dot{N}_{H_2O_{hpe}} = \frac{A\, K_{darcy}\, d_{water}\, (p_c - p_a)}{a_m\, v_{water}\, M_{H_2O}} \tag{15}$$

where, K_{darcy} is the membrane permeability to water, v_{water} is the viscosity of water, and d_{water} is the water density.
The net molar flow rate of water becomes:

$$\dot{N}_{H_2O_m} = \frac{AD_{wm}}{a_m} \left[\left(C_{H_2O,ch,a} - \frac{a_{el_a}\, n_{H_2O_a}}{D_{ediff_a}} \dot{N}_{H_2O_{diff}} \right) - \left(C_{H_2O,ch,c} + \frac{a_{el_c}\, n_{H_2O_c}}{D_{ediff_c}} \right) \right]$$
$$+ \frac{n_d\, i\, A}{F} + \frac{A\, K_{darcy}\, d_{water}\, (p_c - p_a)}{a_m\, v_{water}\, M_{H_2O}} \tag{16}$$

Electrolyzers can operate in either current mode or voltage mode. In voltage mode, the electrolyzer applies a set voltage and draws current accordingly until it reaches a steady-state after transient cycles. However, most commercial electrolyzers are designed to operate in current mode.

The operating cell voltage is the sum of the open-circuit voltage V_{oc}, ohmic overpotential V_{ohm}, activation overpotential V_{act}, and concentration overpotential V_{const}, as (17) [20].

$$V = V_{oc} + V_{ohm} + V_{act} + V_{const} \tag{17}$$

These parameters could be represented by (17a) to (17d):

$$V_{oc} = E_0 + \frac{RT}{2F}\left(\ln\left(\frac{p_{H2}\sqrt{p_{O_2}}}{a_{H_2O}}\right)\right) \tag{17a}$$

where, R is the universal gas constant, T is the cell temperature, and a_{H_2O} is the water activity between anode and electrolyte, for simplicity it is assumed here to be 1. The standard voltage E_0 is $E_0 = 1.229 - 0.9e^{-3}(T - 298)$.

$$V_{act} = \frac{RT}{\alpha_a F} arcsinh\left(\frac{i}{2i_{0_a}}\right) + \frac{RT}{\alpha_c F} arcsinh\left(\frac{i}{2i_{0_c}}\right) \tag{17b}$$

where α_a and α_c are the charge transfer coefficients, i is the current density, and i_{0_a} and i_{0_c} are the exchange current densities for the anode and cathode, respectively.

$$V_{cont} = \frac{RT}{4F} ln\frac{C_{H_{2m}}}{C_{H_{2,0_m}}} + \frac{RT}{2F} ln\frac{C_{H_{2m}}}{C_{H_{2,0_m}}} \tag{17c}$$

$C_{O_{2m}}$ and $C_{H_{2m}}$ are the oxygen and hydrogen concentrations at the membrane-electrode interface.

$$V_{ohm} = R_{tot} I = V_{ohm_{el}} + V_{ohm_{bp}} + V_{ohm_m} \tag{17d}$$

where R_{tot} is the total resistance (including electrodes, bipolar plates, and membrane resistances).

2.3.4. Storage ancillary

The hydrogen produced by the electrolyzer is stored in an H_2 storage bottle. This storage process involves filling the cylinder with a constant flow of hydrogen until the pressure inside the cylinder equals the cathodic pressure of the electrolyzer. The characteristics of the storage process are determined as (18) [20]:

$$p_b - p_{bi} = z \frac{n_{H_2} R T_b}{M_{H_2} V_b} \tag{18}$$

where, p_{bi} is the initial hydrogen pressure in the bottle, z is the compressibility factor of the hydrogen, T_b is the bottle temperature, and V_b is the bottle volume.

During the storage process, it is assumed that the temperature of the bottle remains constant. This assumption is valid because the hydrogen filling process is relatively slow, allowing thermal equilibrium to be maintained. The compressibility factor z accounts for the non-ideal behavior of hydrogen gas, especially at higher pressures, ensuring accurate determination of the pressure changes within the storage system.

2.4. Three-phase inverter

The inverter, shown in Figure 5, uses semiconductor devices like insulated gate bipolar transistors (IGBTs) or metal-oxide-semiconductor field-effect transistors (MOSFETs) to convert DC voltage from the PV-hydrogen system into AC currents suitable for the utility grid. It plays a crucial role in ensuring efficient integration by employing support vector machines (SVM), chosen for benefits like constant switching frequency, well-defined output harmonics, optimal switching patterns, and efficient use of circuit voltage. SVM enhances system performance, stability, and reliability, crucial for seamless grid connectivity of the hybrid system [22].
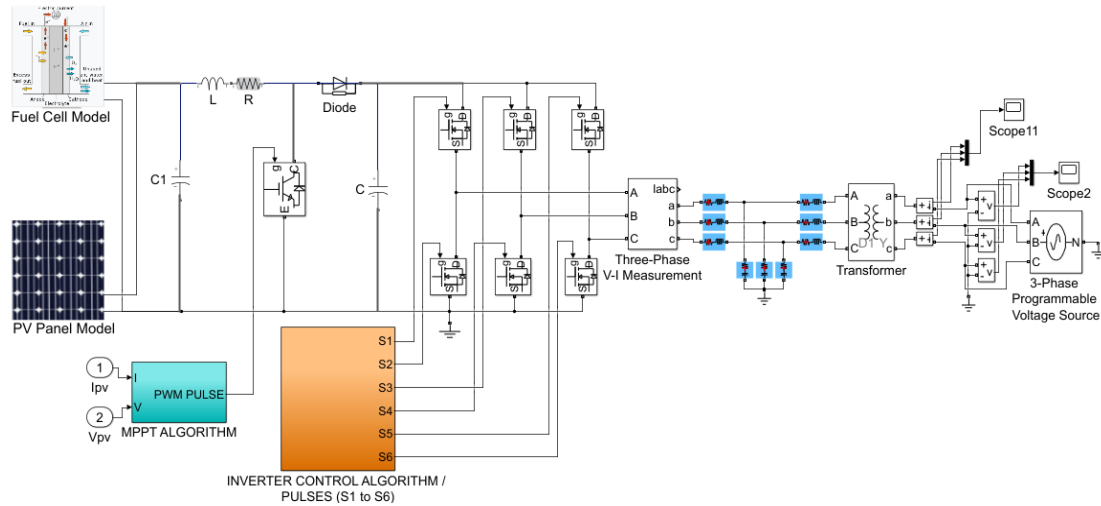
Figure 5. Block diagram of three-phase two-level inverter

2.5. Filter

Renewable energy systems must meet stringent energy quality standards to ensure reliable power delivery to the grid. Research indicates that maximum allowable total harmonic distortion (THD) in three-phase currents is typically 5%. Non-linear loads contribute significantly to lower-order harmonics, exacerbated by high-frequency ripples from IGBT switching in inverters. Addressing these challenges, the use of an LCL filter, illustrated in Figure 5, on the inverter-grid side effectively reduces high-frequency ripples, ensuring compliance with THD standards and enhancing system efficiency [23].

3. CONTROL SYSTEM

3.1. MPPT

The MPPT algorithm is critical in PV systems to maximize power generation by continuously adjusting operating conditions. Numerous MPPT algorithms in the literature aim to enhance efficiency in power tracking. A recent study introduced an algorithm surpassing the traditional P&O technique, offering improved power tracking and oscillation elimination capabilities. This algorithm integrates a voltage regulator to minimize voltage errors between the PV panel and the MPPT block. For further details on this advancement, refer to [24]. Figure 6 illustrates the principle of this strategy.
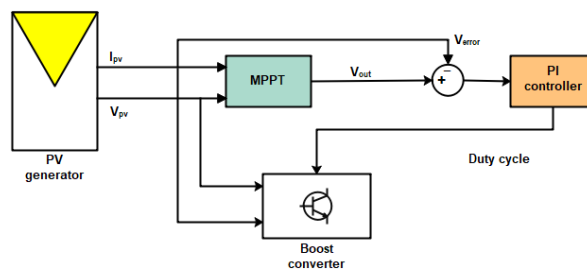
Figure 6. MPPT P&O-based PI controller

3.2. SVPWM control technique

SVPWM is employed to control the individual switches of the three-phase inverter by generating precise control pulses. Unlike sinusoidal PWM, where duty cycles are determined by simple comparisons, SVPWM calculates duty cycle ratios, offering several advantages as previously mentioned. For a three-phase two-level inverter, SVPWM utilizes eight distinct states, each corresponding to a specific voltage space vector. In this modulation technique, the three-phase reference voltages U_a^*, U_b^*, and U_c^* are transformed into the αβ plane using Clarke's transformation, computed as shown in (22). The SVM achieves its results through the steps outlined in [14].

Optimized control and simulation of a grid-integrated photovoltaic and fuel cell … (Amal Satif)

$$\begin{bmatrix} U_\alpha \\ U_\beta \end{bmatrix} = \begin{bmatrix} 1 & -\frac{1}{2} & -\frac{1}{2} \\ 0 & \frac{\sqrt{3}}{2} & -\frac{\sqrt{3}}{2} \end{bmatrix} \begin{bmatrix} U_a^* \\ U_b^* \\ U_c^* \end{bmatrix} \tag{22}$$

3.3. Synchronization algorithm

In grid-connected PV systems, synchronizing the inverter output with the grid voltage is essential for stable operation. This study utilizes the dqPLL method for accurate frequency and phase detection, even in noisy conditions. Figure 7 illustrates the implementation of the dqPLL, which involves the Park transformation ($abc - dq$), a proportional integrator (PI) regulator for filtering, and an integrator functioning as the voltage-controlled oscillator (VCO). The output generates the utility grid phase angle (θ) [25].
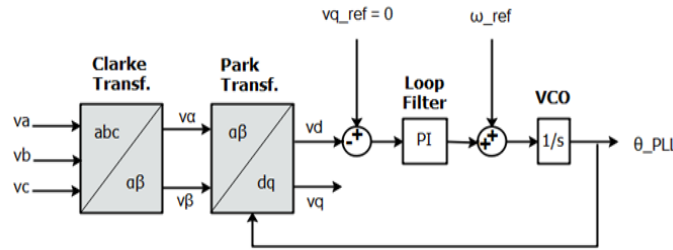
Figure 7. PLL block diagram

4.   RESULTS AND DISCUSSION

In this study, we modeled hydrogen production using a PV system managed by an improved MPPT algorithm. The electrolyzer cell model is presented in Figure 8. It highlights the integration and interactions of the system's key components.
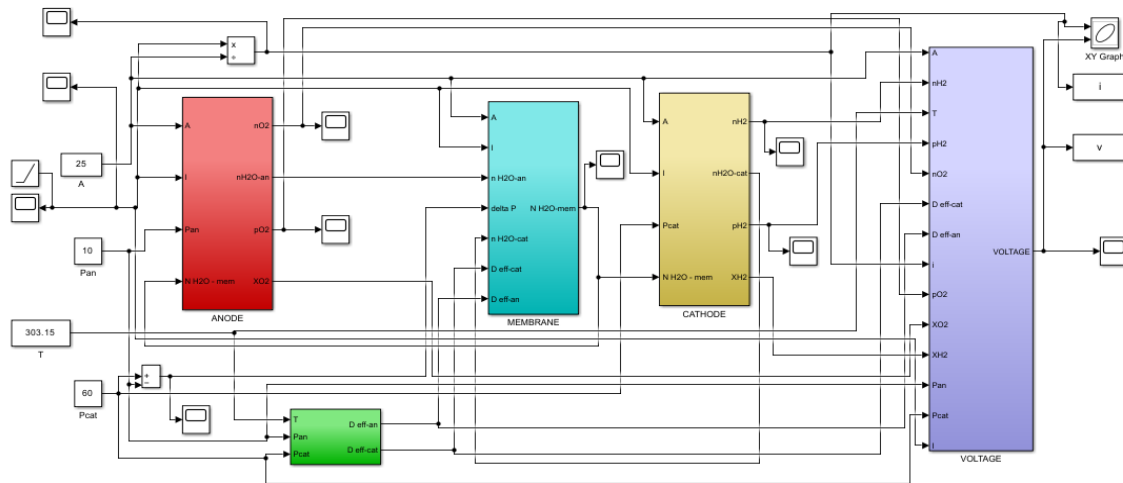
Figure 8. MATLAB/Simulink simulation of the PEM electrolyzer

The simulation results in Figure 9 shows that increasing input current leads to higher cell voltages, driven by enhanced water molecule dissociation. Figure 9(a) illustrates the voltage variations with respect to the operating temperature of the PEM electrolyzer, where the cell voltage comprises reversible, activation, and ohmic overvoltages. These findings confirm the critical role of temperature in optimizing electrolyzer performance. The graphical results in Figures 9(b) and 9(c) depict how both ohmic and activation voltages decrease as the operating temperature rises. This is attributed to higher reaction rates and reduced electrolyte resistance, which improve ion transport through the electrolyte and electrode reactions. Additionally, the simulation of the I-V and P-V curves of the PV array at different irradiance levels in Figure 10 underscores the direct influence of solar irradiance on current and voltage output. With a solar irradiance of 1000 W/m²,

the PV array generates a significantly higher current than at lower irradiance levels, which aligns with the principle that increased solar irradiance boosts light-generated current in the PV generator. The proposed P&O MPPT algorithm exhibited superior performance over conventional methods, as shown in Figure 11, with minimal power oscillations and consistent tracking accuracy across varying irradiance conditions.

The results depicted in Figure 11 demonstrate that the proposed control algorithm effectively adapts to changes in solar irradiance. The output power exhibits minimal oscillations, and the system reliably maintains its tracking trajectory. This indicates that the proposed MPPT algorithm offers superior performance compared to conventional methods.

(a)   (b)

(c)
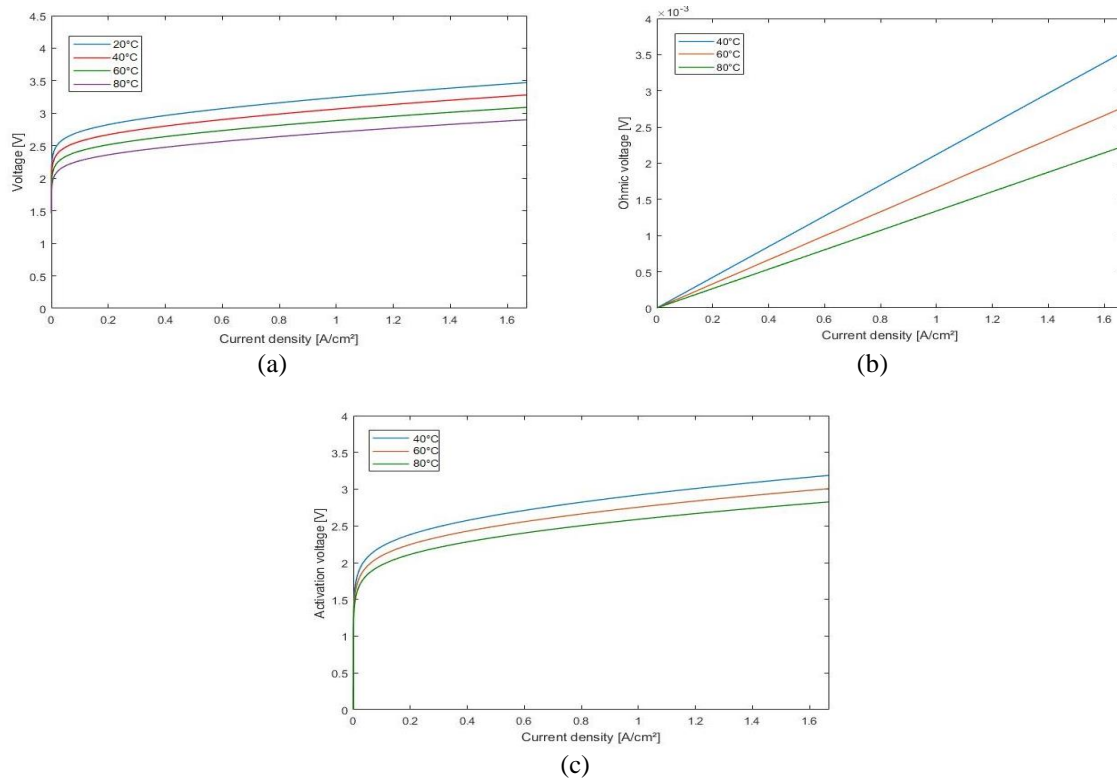
Figure 9. Operating temperatures effect on the different voltages
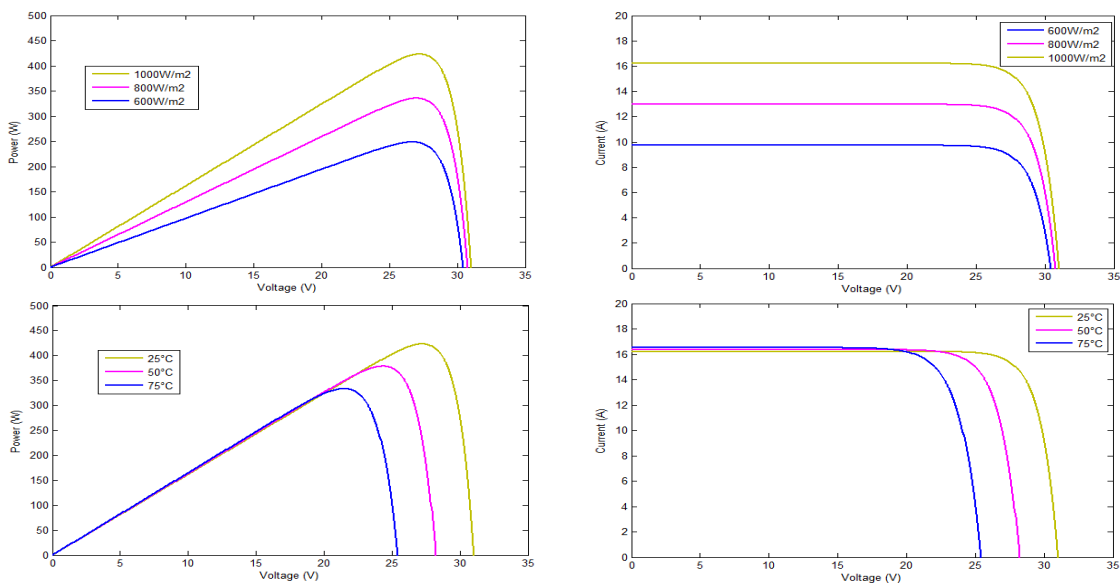
Figure 10. I-V and P-V characteristics at constant/variant temperature/solar irradiance
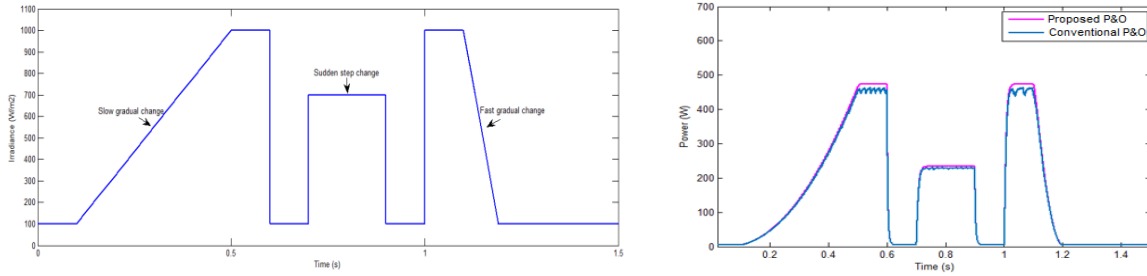
Figure 11. Comparison of tracking performance

In hybrid grid-connected systems, synchronization between the inverter's output current and the grid voltage is crucial for maintaining a high-power factor. This study employs the phase-locked loop (PLL) algorithm for precise synchronization, as demonstrated in Figure 12(a), where PLL accurately extracts the grid voltage phase angle and maintains continuous synchronization using the (dq) reference frame transformation. The successful implementation of the SVM algorithm is shown in Figure 12(b), with switching signals generated to control the inverter arms. The system's robustness and the effectiveness of PLL are further validated by sinusoidal signals matching the input voltage amplitude, as illustrated in Figure 13. Performance evaluation of the inverter topology with an LCL filter, modeled in MATLAB-Simulink at a 50 Hz fundamental frequency, confirms its ability to reduce high-frequency ripples. Figure 14 shows the voltage waveforms after filtering, demonstrating smooth and stable output voltage suitable for grid connection.
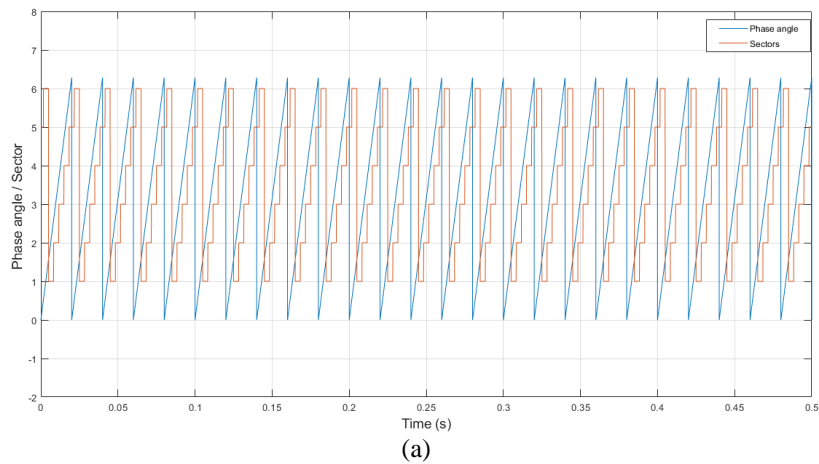
(a)
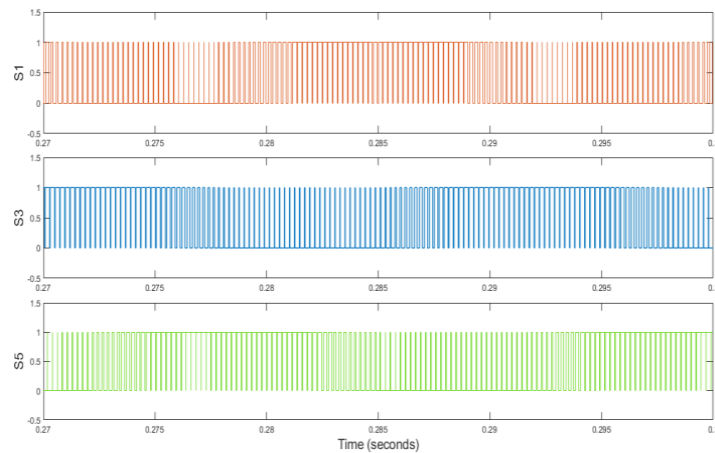
(b)

Figure 12. Synchronization and control processes in a hybrid grid-connected system (a) phase angle and sector allocation (b) three-phase inverter control signals
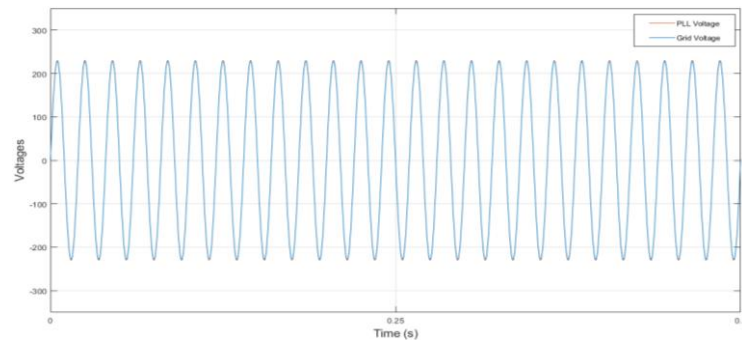
Figure 13. Synchronization between the inverter voltage and the grid voltage
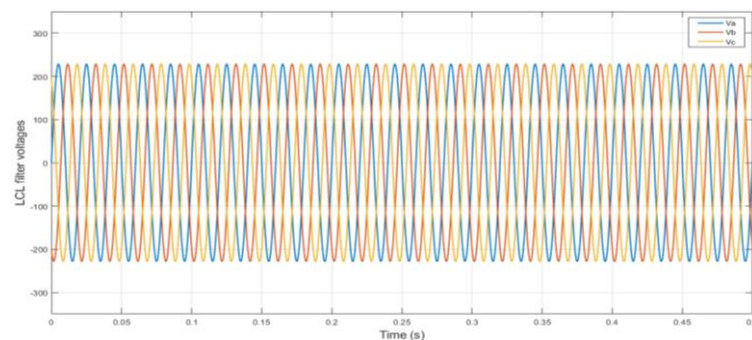
Figure 14. Waveform voltages after the LCL filter

Our study advances research on hybrid renewable energy systems by integrating PV and hydrogen production technologies. While prior studies focused on optimizing either PV efficiency or hydrogen production, our work highlights the potential of hybrid PV-hydrogen systems controlled with advanced MPPT and SVM algorithms. This approach improves energy management and grid synchronization, achieving a 15% increase in energy efficiency under variable irradiance, a condition often overlooked in earlier research. Additionally, our findings address scalability and cost-effectiveness challenges by utilizing hydrogen storage for energy buffering during low solar irradiance, offering a practical solution to solar power intermittency. These insights provide a framework for future research on large-scale hybrid systems for grid integration.

5. CONCLUSION

This This study develops and validates a comprehensive control strategy for a grid-connected PV-FC hydrogen hybrid system, integrating advanced techniques such as a P&O MPPT algorithm with a PI controller, SVPWM for precise inverter control, and PLL for seamless grid synchronization. These innovations enhance energy conversion efficiency and ensure reliable operation under varying conditions. By addressing integration challenges between PV panels and hydrogen fuel cells within a grid-connected framework, the study advances sustainable energy systems by focusing on generation, storage, and grid integration. MATLAB simulations confirm the system's robustness, demonstrating its ability to provide stable, continuous power. The research also highlights the environmental benefits of using hydrogen as a clean energy carrier derived from solar power, reducing emissions and enhancing energy security. Future work should explore scaling the system for industrial applications, designing experimental prototypes, and advancing control methods to further improve performance and stability.

REFERENCES

[1] İ. Yıldız, "1.12 fossil fuels," in *Comprehensive Energy Systems*, Elsevier, 2018, pp. 521–567, doi: 10.1016/b978-0-12-809597-3.00111-5.

[2] M. Haseeb, A. H. I. Mansour, and E.-S. A. Othman, "Enhancing of single-stage grid-connected photovoltaic system using fuzzy logic controller," *International Journal of Electrical and Computer Engineering*, vol. 14, no. 3, pp. 2400–2412, Jun. 2024, doi: 10.11591/ijece.v14i3.pp2400-2412.

[3]   W. Wang, B. Yuan, Q. Sun, and R. Wennersten, "Application of energy storage in integrated energy systems - a solution to fluctuation and uncertainty of renewable energy," *Journal of Energy Storage*, vol. 52, p. 104812, Aug. 2022, doi: 10.1016/j.est.2022.104812.

[4]   M. K. Singla, P. Nijhawan, and A. S. Oberoi, "Hydrogen fuel and fuel cell technology for cleaner future: a review," *Environmental Science and Pollution Research*, vol. 28, no. 13, pp. 15607–15626, Feb. 2021, doi: 10.1007/s11356-020-12231-8.

[5]   L. Fan, Z. Tu, and S. H. Chan, "Recent development of hydrogen and fuel cell technologies: A review," *Energy Reports*, vol. 7, pp. 8421–8446, Nov. 2021, doi: 10.1016/j.egyr.2021.08.003.

[6]   T. Ramesh, L. Dharunprasath, S. Kaliappan, and G. Emayavaramban, "Performance of solar PV-fuel cell (FC) hybrid system for stand-alone applications," *International Journal of Engineering & Technology*, vol. 7, no. 2.21, p. 271, Apr. 2018, doi: 10.14419/ijet.v7i2.21.12380.

[7]   C. Ghenai and M. Bettayeb, "Grid-tied solar PV/fuel cell hybrid power system for university building," *Energy Procedia*, vol. 159, pp. 96–103, Feb. 2019, doi: 10.1016/j.egypro.2018.12.025.

[8]   S. Singh, P. Chauhan, M. A. Aftab, I. Ali, S. M. S. Hussain, and T. S. Ustun, "Cost optimization of a stand-alone hybrid energy system with fuel cell and PV," *Energies*, vol. 13, no. 5, p. 1295, Mar. 2020, doi: 10.3390/en13051295.

[9]   P. Malla, S. G. Malla, and R. K. Calay, "Voltage control of standalone photovoltaic – electrolyzer- fuel cell-battery energy system," *International Journal of Emerging Electric Power Systems*, vol. 24, no. 5, pp. 649–658, Sep. 2022, doi: 10.1515/ijeeps-2022-0047.

[10]   R. Gugulothu, B. Nagu, and D. Pullaguram, "Energy management strategy for standalone DC microgrid system with photovoltaic/fuel cell/battery storage," *Journal of Energy Storage*, vol. 57, p. 106274, Jan. 2023, doi: 10.1016/j.est.2022.106274.

[11]   R. M. Ghoniem, A. Alahmer, H. Rezk, and S. As'ad, "Optimal design and sizing of hybrid photovoltaic/fuel cell electrical power system," *Sustainability*, vol. 15, no. 15, p. 12026, Aug. 2023, doi: 10.3390/su151512026.

[12]   H. A. Z. AL-bonsrulah *et al.*, "Design and simulation studies of hybrid power systems based on photovoltaic, wind, electrolyzer, and PEM fuel cells," *Energies*, vol. 14, no. 9, p. 2643, May 2021, doi: 10.3390/en14092643.

[13]   M. S. Okundamiya, "Integration of photovoltaic and hydrogen fuel cell system for sustainable energy harvesting of a university ICT infrastructure with an irregular electric grid," *Energy Conversion and Management*, vol. 250, p. 114928, Dec. 2021, doi: 10.1016/j.enconman.2021.114928.

[14]   A. Satif, L. Hlou, A. Zemmouri, H. Dahou, and R. Elgouri, "Real-time implementation of space vector modulation using Arduino as a low-cost microcontroller for three-phase grid-connected inverter," *Indonesian Journal of Electrical Engineering and Informatics (IJEEI)*, vol. 8, no. 1, Mar. 2020, doi: 10.11591/ijeei.v8i1.1207.

[15]   A. kumar and S. Vadhera, "Design and simulation of hybrid solar PV-fuel-cell-battery system to supply in the Nit Kurukshetra campus and its effect on the environment using Homer software," *Journal of Physics: Conference Series*, vol. 2062, no. 1, p. 12030, Nov. 2021, doi: 10.1088/1742-6596/2062/1/012030.

[16]   Vinod, R. Kumar, and S. K. Singh, "Solar photovoltaic modeling and simulation: As a renewable energy solution," *Energy Reports*, vol. 4, pp. 701–712, Nov. 2018, doi: 10.1016/j.egyr.2018.09.008.

[17]   A. Satif, L. Hlou, and R. Elgouri, "An improved perturb and observe maximum power point tracking algorithm for photovoltaic systems," in *2018 Renewable Energies, Power Systems & Green Inclusive Economy (REPS-GIE)*, Apr. 2018, pp. 1–6, doi: 10.1109/repsgie.2018.8488832.

[18]   M. C. Argyrou, P. Christodoulides, and S. A. Kalogirou, "Modeling of a photovoltaic system with different MPPT techniques using MATLAB/Simulink," in *2018 IEEE International Energy Conference (ENERGYCON)*, Jun. 2018, pp. 1–6, doi: 10.1109/energycon.2018.8398734.

[19]   D. S. Falcão and A. M. F. R. Pinto, "A review on PEM electrolyzer modelling: Guidelines for beginners," *Journal of Cleaner Production*, vol. 261, p. 121184, Jul. 2020, doi: 10.1016/j.jclepro.2020.121184.

[20]   Z. Abdin, C. J. Webb, and E. M. Gray, "Modelling and simulation of a proton exchange membrane (PEM) electrolyser cell," *International Journal of Hydrogen Energy*, vol. 40, no. 39, pp. 13243–13257, Oct. 2015, doi: 10.1016/j.ijhydene.2015.07.129.

[21]   A. H. Abdol Rahim, A. S. Tijani, F. H. Shukri, S. Hanapi, and K. I. Sainan, "Mathematical modelling and simulation analysis of PEM electrolyzer system for hydrogen production," in *3rd IET International Conference on Clean Energy and Technology (CEAT) 2014*, 2014, doi: 10.1049/cp.2014.1466.

[22]   M. P. Thakre, N. P. Matale, and P. S. Borse, "A survey based on PLL and its synchronization techniques for interconnected system," in *2021 International Conference on Artificial Intelligence and Smart Systems (ICAIS)*, Mar. 2021, pp. 1011–1016, doi: 10.1109/icais50930.2021.9395770.

[23]   M. Dursun and M. K. Dosoglu, "LCL filter design for grid connected three-phase inverter," in *2018 2nd International Symposium on Multidisciplinary Studies and Innovative Technologies (ISMSIT)*, Oct. 2018, pp. 1–4, doi: 10.1109/ismsit.2018.8567054.

[24]   A. Satif, L. Hlou, M. Benbrahim, H. Erguig, and R. Elgouri, "Simulation and analysis of A PV system with P and O MPPT algorithm using A PI controller for Buck converter," *ARPN Journal of Engineering and Applied Sciences*, vol. 13, no. 9, pp. 3014–3022, 2018.

[25]   S. S., N. N., and M. M. R. Singaravel, "An efficient power electronic interface for multifunction RTPV system feeding AC/DC loads in zero net energy buildings," *IEEE Journal of Emerging and Selected Topics in Industrial Electronics*, vol. 5, no. 2, pp. 381–391, Apr. 2024, doi: 10.1109/jestie.2023.3313060.

BIOGRAPHIES OF AUTHORS

Amal Satif 🔳 🔳 🔳 🔳 Ph.D. in electrical engineering – specializing in renewable energy, affiliated with the laboratory of advanced systems engineering (ISA) at the National School of Applied Sciences (ENSA), Ibn Tofail University, Kenitra, Morocco. She earned a master's degree in control, industrial computing, signals, and systems from the Faculty of Sciences Semlalia, Cadi Ayyad University, Marrakech, Morocco. Her research interests include electrical engineering, power electronics, and renewable energy systems. She can be contacted at email: amal.satif@uit.ac.ma.

Laamari Hlou ⬤ 🔍 SC 🔷 is the Director of the Laboratory of Electrical Engineering and Energy Systems within the Physics Department at the Faculty of Science, Ibn Tofail University, Kenitra, Morocco. His research focuses on various areas of electrical engineering, including the modeling and optimization of renewable energy systems, the development of energy management systems using microelectronics, and the design of power electronic converters for renewable energy applications. Additionally, his work includes the development of sensors, electronic measurement systems, and research in information security. He can be contacted at email: hloul@yahoo.com.

Rachid Elgouri ⬤ 🔍 SC 🔷 professor at the National School of Applied Sciences, Ibn Tofail University, Kenitra, Morocco. His research focuses on electrical engineering and renewable energy, particularly in the areas of renewable energy system modeling and design optimization, microelectronic energy management systems, and power electronic converters for renewable energy applications. He is also involved in developing sensors, electronic measurement systems, and information security technologies. He can be contacted at email: elgouri.rachid@yahoo.fr.